Environ. Sci. Technol. **2010,** *44,* 1736–1741

Rapid and Sensitive Detection of *Giardia lamblia* Using a Piezoelectric Cantilever Biosensor in Finished and Source Waters

SEN XU AND RAJ MUTHARASAN*

Department of Chemical and Biological Engineering, Drexel University, Philadelphia, Pennsylvania 19104

Received November 9, 2009. Revised manuscript received January 15, 2010. Accepted January 21, 2010.

The current method for detecting the waterborne parasite *Giardia lamblia* is tedious and requires a preconcentration step. We show for the first time a piezoelectric-excited millimeter-sized cantilever (PEMC) biosensor immobilized with a monoclonal antibody against *G. lamblia* that exhibits selective and sensitive detection of *G. lamblia* cysts in several water matrixes (buffer, tap, and river water) at a detection limit of 1−10 cysts/mL without a preconcentration step. The PEMC sensor is a resonance-based device that functions at a high-order mode near 1 MHz. The antibody-immobilized sensor was exposed to 1−10,000 *G. lamblia* cysts/mL samples in a flow arrangement. When the cysts bind to the antibody on the sensor, the resonant frequency of the cantilever sensor decreases and is recorded continuously. Positive confirmation of sensor detection responses was obtained by environmental scanning electron microscope of sensor surface after detection experiments. Higher sample flow rates (0.5−5.0 mL/min) gave higher sensor detection response. Detecting as few as 10 cysts per mL was achieved in all three water matrixes tested, and significant sensor response was obtained in 15 min. We also show the feasibility of analyzing at a low concentration of 1 cyst/mL in a one liter sample at a high flow rate of 5 mL/min.

1. Introduction

Giardia lamblia is a flagellated enteric protozoan parasite and a causative agent of human giardiasis (*1*). Giardiasis causes acute or chronic diarrhea, asymptomatic illness and severe malabsorption resulting in weight loss, and is frequently implicated in waterborne outbreaks. Infection occurs by ingestion of *G. lamblia* cysts present in contaminated water and food, or by fecal−oral route (*2*). Together with *Cryptosporidium*, *Giardia* has been classified as one of the important pathogens in the WHO Neglected Disease Initiative (*3*). Since ingestion of as few as ten cysts may cause giardiasis, there is a great need for a sensitive method for detecting and monitoring *G. lamblia* in source and finished drinking water samples.

U.S. Environmental Protection Agency (EPA) established Method 1623 for detection of both *Cryptosporidium* and *Giardia* simultaneously. This method requires filtration of a large water sample, followed by immunomagnetic capture and separation, and subsequent immunofluorescence labeling and microscopic enumeration (*4*). To reduce time of analysis, alternate methods such as polymerase chain reaction (PCR) and enzyme-linked immunosorbent assay (ELISA) have been investigated (*5–8*). Although PCR is extremely sensitive (1−10 cysts), it requires a preconcentration step following the filtration step. ELISA, on the other hand, exhibits poor sensitivity (10^4 to 10^5 cysts). Although several advanced methods have been investigated for *G. lamblia* detection, they are either tedious or exhibit poor sensitivity (*9–11*). On the other hand, cantilever biosensors have exhibited high sensitivity and selectivity for pathogen detection (*12, 13*). Since they are responsive to mass-change at femtogram levels in liquid, we examine the applicability of the cantilever sensors for detecting *Giardia* cysts. Unlike bacterial pathogens the cysts are large, and no antibody-based biosensor method has been reported for *G. lamblia* detection. This we believe is in part due to their size as it is considerably larger (∼10 μm) than bacterial pathogens (∼1 μm). While quartz crystal microbalance (QCM) and similar resonators have been found to exhibit sensitivity at nanogram levels for molecules, they exhibit poor detection limit for *Cryptosporidium parvum* (10^5 oocysts/mL) which is larger (∼3 μm) than a bacterium, but smaller than *Giardia* (*14*). In our earlier work we showed piezoelectric-excited millimeter-sized cantilever (PEMC) sensor was sensitive and showed detection of *C. parvum* at 100 oocysts/mL in clean buffers (*15*). In this paper, we examine if antibody-immobilized PEMC sensors exhibit detection sensitivity at a much lower concentration of *G. lamblia* cysts in practical water matrixes of tap water and river water. We also show successful detection of cysts in 1 L samples at a flow rate of 5.0 mL/min. The latter is significant as most biosensor assays are carried out at low flow rates; for example, surface plasmon resonance (SPR) and QCM operate typically at 10−100 μL/min. Studies on high flow rate detection with biosensors are few. In one study with 55 MHz QCM for protein detection flow rate was found to give a larger overall sensor response (*16*). Higher flow rate sensing is advantageous because a larger sample volume can be analyzed without a preconcentration step.

2. Experimental Section

2.1. PEMC Sensor. PEMC sensor is a cantilever sensor that measures mass-change by change in resonant frequency. It is composed of a PZT layer and a glass layer. A detailed description of cantilever physics can be found in (*17*). For cantilever biosensors that operate in resonant (dynamic) mode, resonant frequency decrease is caused by binding of cysts to antibody-immobilized cantilever surface.

2.2. Experimental Details. Detailed materials and methods are provided in the Supporting Information (SI). Briefly, fabricated sensors were gold coated, incubated sequentially in cysteamine and glutaraldehyde, and then installed in a custom-made flow cell connected to running buffer and sample reservoirs (flow apparatus schematic is given in SI Figure S1) (*18*). Resonant frequency of the sensor was monitored continuously. Antibody against *Giardia* was circulated across the sensor until immobilization on sensor was complete as indicated by its resonant frequency reaching a constant value. Subsequently, samples containing known *G. lamblia* cysts were injected into the flow loop in recirculation mode until resonant frequency reached a new steady state following a detection response. Tap water was obtained locally and river surface water was collected from the Schuylkill River near 30th and Market St. in Philadelphia, PA. Both water samples were used as collected without any filtration or treatment.

* Corresponding author tel: (215) 895-2236; fax: (215) 895-5837; e-mail: mutharasan@drexel.edu.

10.1021/es9033843
Published on Web 02/03/2010

3. Results and Discussion

3.1. Sensor Characteristics. A set of PEMC sensors ($m = 10$) with similar spectral property was used in the detection experiments. All sensors were fabricated with exposed dimensions of 2.0 × 1.0 mm glass layer and 2.7 × 1.0 mm ($l \times w$) PZT layer. They exhibited a dominant resonant mode in the 920−950 kHz frequency range. All sensors showed similar frequency shift for air-to-water transition of 64.50 ± 5.50 kHz, and we interpret this response as an approximate measure of sensitivity to mass-change.

The frequency spectrum of a typical PEMC sensor in air and in flow cell at 5.0 mL/min is given in Figure S2. The sensor exhibited resonant frequency at 930.75 kHz in air and 869.25 kHz in liquid, which is a frequency shift $\Delta f = 61.50$ kHz. Quality factor (Q-factor, a measure of peak shape) of the sensor decreased from 31 in air to 26 in liquid, and is a modest decrease of ~16%. The robustness of Q-factor in liquid renders the PEMC sensor an effective device for direct in-liquid application and measurement. Since we examine in this paper flow rate effects on sensor response to cyst binding, we first investigated the effects of flow rate on sensor resonant frequency dynamics. In this case, an unfunctionalized sensor was installed in the flow apparatus and the flow rate was changed from 0.8 to 5.0 mL/min. At this flow rate the average velocity in the flow cell was 0.46 cm/s and the flow was laminar at a Reynolds number of 22. The resonant frequency decreased by ~200 Hz in an almost step-like manner and then stabilized rapidly at the new higher flow rate of 5.0 mL/min (see Figure S2). The noise level of measured sensor resonant frequency increased from ±10 to ±38 Hz following the flow rate increase. The Q-factor did not change (<2%) when flow rate was changed from 0.8 to 5.0 mL/min. The data in Figure S2 show that continuous monitoring of resonant frequency at 5.0 mL/min in the flow cell was feasible. Stability of sensor resonant frequency at such a high flow velocity indicates the robustness of the sensor and is an attractive characteristic of PEMC sensor.

3.2. Sequential Detection Using PEMC Sensor. Sequential detection experiments to increasing cyst concentration were first carried out to examine antibody binding affinity and detection sensitivity for *G. lamblia* cysts. In Figure 1, we show a sequential detection experiment conducted at 0.8 mL/min. The gold-coated sensor was functionalized by incubating in cysteamine and glutaraldehyde, and then was exposed it to antibody in the flow loop set in recirculation mode. As can be seen in Figure 1, the resonant frequency showed a gradual decrease of 575 ± 5 Hz as antibody immobilization occurred via the surface aldehyde group. After steady state was reached, indicating completion of antibody immobilization, various concentration samples of *G. lamblia* from 10 to 10,000 cysts/mL were injected into the flow loop set in recirculation mode. Recirculation was found to be necessary as a 1 mL sample at 0.8 mL/min did not provide sufficient time for binding. After each injection sufficient time was allowed for binding reaction to occur and was assessed by the sensor resonant frequency reaching a steady state value. Frequency responses to sequential addition of increasing number of cysts—10, 100, 1,000, and 10,000 gave frequency shifts of 67, 650, 490, and 360 Hz, respectively. Addition of a further 10,000 cysts sample gave a modest frequency decrease of 120 Hz, and the low response may suggest limitation of available antibody sites on the sensor. The functionalized sensor surface area was 2 mm^2, and if it were covered entirely with cysts (~12 μm long and ~6 μm wide, see Figure S3), the sensor could accommodate a maximum of ~30,000 cysts. The actual number captured by a sensor is likely to be a fraction of this value due to steric effects and nonuniform surface antibody distribution. Therefore a low response for 10,000 cysts after an exposure to 1,110 cysts could be attributed to availability of binding sites.

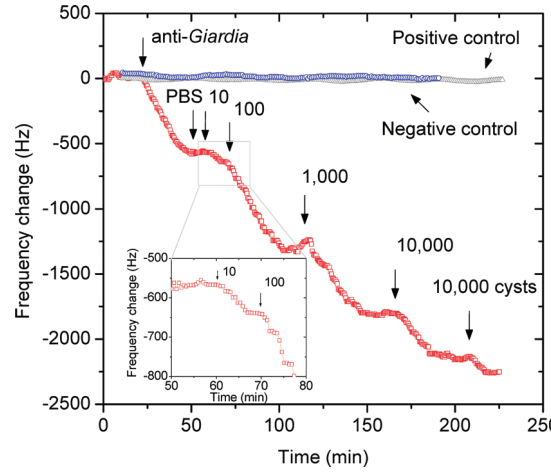

FIGURE 1. Sequential detection of *G. lamblia* cysts in PBS at 0.8 mL/min. After sensor was prepared with an exposed aldehyde group, it was installed in the flow cell with PBS as running buffer. Anti-*Giardia* (10 μg/mL) was injected in and the flow was set in recirculation mode for antibody reaction to surface aldehyde group. As reaction occurred, resonant frequency decreased and reached a steady state. After a PBS rinse step, sequential cysts addition to the flow loop was made allowing for the sensor to reach steady state following each addition. Inset shows an expanded response for a 10 cysts sample.

The infectious dose of *G. lamblia* cysts has been reported to be as low as 10−25 cysts (*19*), which means for a biosensor to be of practical use, the limit of detection should be less than 10 cysts. Experiments at 0.8 mL/min showed the potential for detecting 10 cysts. The response was 81 ± 19 Hz ($n = 5$). Compared with the average noise level (18 ± 3 Hz) at 0.8 mL/min, the response to 10 cysts detection exhibited a signal-to-noise ratio (S/N) of 4.5. Even though positive response to 10 cysts was obtained, the S/N was modest for confident screening of samples. To improve the performance of PEMC sensor for low concentration detection, we investigated sample flow rate effects on the total sensor response. Our underlying hypothesis was the sensor response was limited by cyst transport rate to sensor surface. It is important to remember that we rely on fluid flow to transport cysts to the vicinity of sensor surface. The immobilized antibody does not attract the cysts. Further the cysts have a limited number of antigenic sites that are responsible for binding to sensor. Thus their transport to surface may not be sufficient for binding since we also require the antigenic sites be accessible to the exposed antibody binding region. To examine the validity of flow-field hypothesis, a series of experiments was carried out at a higher flow rate of 2.4 mL/min which is 3 times the flow rate used in Figure 1. The sensor responses obtained to separate exposures of low concentration samples 10−500 cysts given in Figure 2 validates the flow-field hypothesis. Positive control response with an unfunctionalized (no antibody) sensor exposed to 500 cysts in recirculation showed a small response of 10 ± 6 Hz, which is essentially at the noise level. As shown in Figure 2A, for 10, 50, and 500 cysts, the frequency decreases were 190, 450, and 790 Hz, respectively. Responses that were significantly larger than the noise level were observed in the first 10 min. The S/N for 10 cysts detection was greater than 10, which is an improvement over sensor response at 0.8 mL/min. Repeat experiments ($n = 4$) for detecting 10−500 cysts samples were carried out and the average response to each concentration is shown in Figure 2B. One notes the sensitivity of the same sensor can be enhanced by flow rate resulting in improved S/N, and therefore a lower limit of detection was achieved. To confirm that the PEMC sensor

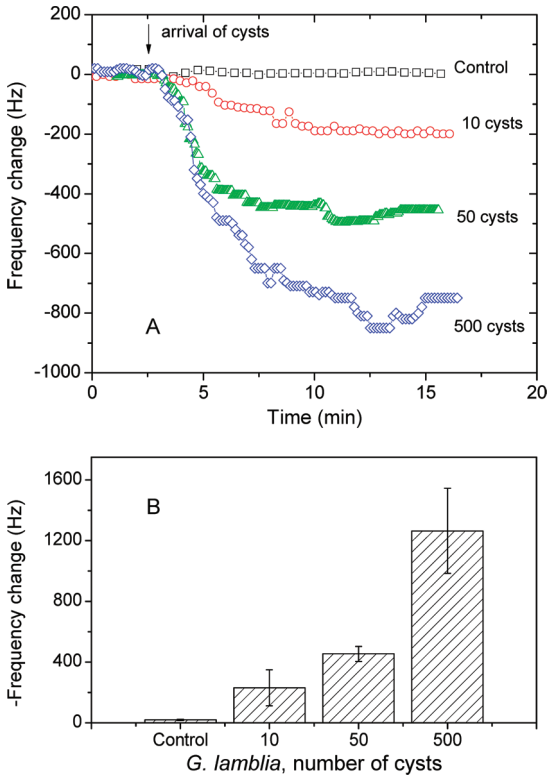

FIGURE 2. (A) Response of the sensor to addition of 1 mL of sample containing 10, 50, and 500 cysts/mL *G. lamblia* samples to the flow loop set in recirculation mode at 2.4 mL/min. (B) Average frequency responses ($n = 4$) to various concentrations at 2.4 mL/min. Negative control experiments showed responses of 20 ± 5 Hz ($n = 4$). Error bars represent one standard deviation ($n = 4$).

response was indeed due to *G. lamblia* binding to the sensor surface, the sensor surface was examined in environmental scanning electron microscope (ESEM) after detection experiments. In Figure S3 we show typical ESEM images of sensor surface taken after a detection experiment in which a cumulative exposure to 11,110 cysts had occurred. Attached cysts were evenly distributed through the 2 mm^2 sensor area, and covered ~5% of the sensor area.

3.3. Effect of Flow Rate on Sensor Response and Quantification. Comparing the results in Figures 1 and 2, one notes the sensor response for the same *G. lamblia* concentration depended on the flow rate used. We examined systematically the effects of flow rate by conducting detection experiments in the range of 0.5−5.0 mL/min and cysts concentrations 10−10,000 cysts/mL. Figure 3 shows the sensor responses to two different *G. lamblia* concentrations: 500 and 10,000 cysts/mL at flow rates of 0.8, 1.5, and 2.4 mL/min. Samples containing 500 cysts gave progressively higher responses of 470, 640, and 790 Hz as the flow rate was increased. Similar experiments with 10,000 cysts gave responses of 1,210, 1,470 and 2,820 Hz, respectively. At both concentrations, the magnitude of response to the same number of cysts increased as the flow rate was increased from 0.8 to 1.5, and then to 2.4 mL/min. Reports on using flow rate as a means to improve biosensor response are few. The likely reason is most biosensor platforms exhibit high measurement noise at high flow rates due to the limitation of sensor flow cell design used. Examples are QCM and SPR which are typically conducted in a flow format at less than 0.1 mL/min. As shown in Figure S2, the PEMC resonant peak shape remained intact at 5.0 mL/min and the noise in resonant frequency measurement was ±38 Hz. We found PEMC sensor to be usable at an even higher flow rate of 17 mL/min, but at a much higher measurement noise. Experi-

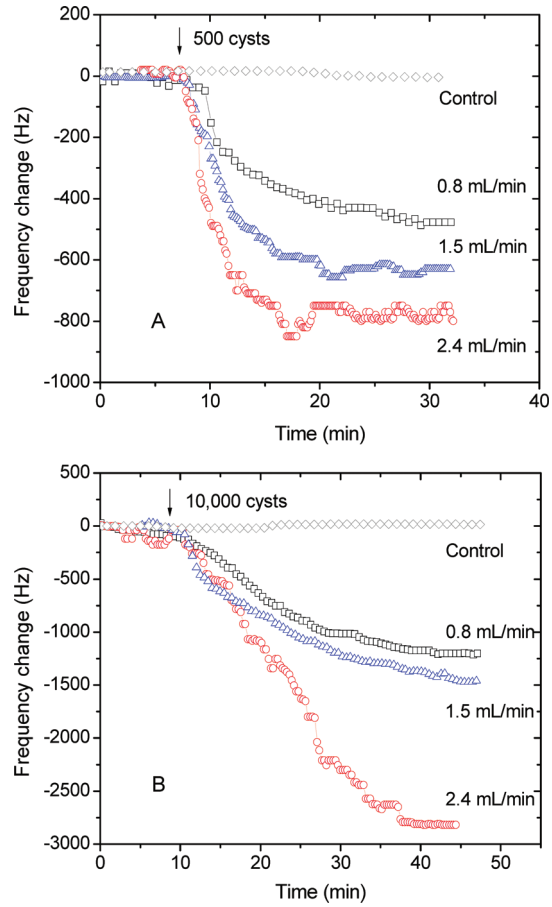

FIGURE 3. Responses of PEMC sensor to (A) 500 cysts and (B) 10,000 cysts at the three flow rates: 0.8, 1.5, and 2.4 mL/min. Higher flow rate resulted in higher magnitude of sensor response. Responses to the positive controls (sensor without antibody) were in the noise level.

mentally 5.0 mL/min was used as an intermediate value for 1 L sample study (Section 3.4) at which continuous monitoring of resonant frequency was obtained at reasonable noise level.

As noted earlier, a group of PEMC sensors with nearly identical geometry was used in the present study. For a biosensor to be useful in practical applications, one important consideration is repeatability of detection responses using different sensors but of same design. We examined the response of a set of different sensors to the same *G. lamblia* concentration at the same assay condition. In earlier studies, we observed sensor resonant frequency decrease correlated with analyte concentration by a log−linear function, $(-\Delta f) = A\ \mathrm{Log}(C) + B$, for the cases of the pathogen *Bacillus anthracis* (*20*), and the toxin staphylococcal enterotoxin B (*21*). The term $(-\Delta f)$ is the steady-state resonant frequency response and C is the concentration of target analyte exposed to the sensor. The parameters A and B are sensor constants which depend on cantilever geometry, antibody−antigen binding constant, and antibody surface concentration.

To examine whether the same relationship noted above holds true for *G. lamblia*, a plot of frequency response to *G. lamblia* cysts concentrations ranging from 10 to 12,500 cysts/mL at three different flow rates (0.5, 0.8, and 2.4 mL/min) using ten different sensors was prepared, and is given in Figure 4. Flow rate of 1.5 mL/min was also investigated, but data are not included here for clarity of presentation. From the plot we see the frequency response obtained using various sensors of same geometric design correlated quite well with log of *G. lamblia* cysts concentration ($n = 3$ for 0.5 mL/min, $n = 3-5$ for 0.8 mL/min, $n = 3-4$ for 2.4 mL/min). The

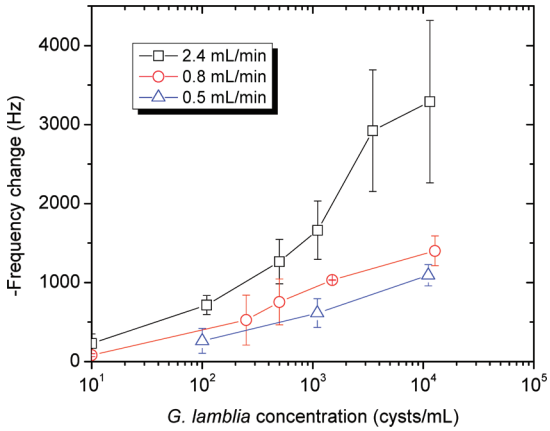

FIGURE 4. Quantification of sensor response using a group of PEMC sensors (m = 10) at the flow rates of 0.5, 0.8, and 2.4 mL/min. Each data point represents an average of a minimum of three experiments. Error bars represent one standard deviation (n = 3–5).

TABLE 1. Effect of Flow Rate on Sensor Response Correlation with *G. lamblia* Concentration

flow rate (mL/min)	correlation	R^2
0.5	$(-\Delta f) = 405.7\ \mathrm{Log}(C) - 572.5$	0.99
0.8	$(-\Delta f) = 435.4\ \mathrm{Log}(C) - 405.9$	0.98
1.5	$(-\Delta f) = 572.3\ \mathrm{Log}(C) - 573.4$	0.92
2.4	$(-\Delta f) = 1055.0\ \mathrm{Log}(C) - 1200.9$	0.91

results indicate good repeatability of experiments using a group of PEMC sensors (m = 10). The experimental data were fitted to the log–linear relationship noted above, and the correlation properties are summarized in Table 1. We note the correlation coefficient decreased from $R^2 = 0.99$ at 0.5 mL/min to R^2 = 0.91 at 2.4 mL/min. Also standard deviation increased with flow rate indicating a higher variance in sensor response. Figure 4 shows higher flow rate enhanced transport and binding of *G. lamblia* to sensor surface quite significantly. The enhancement in sensor response is seen in the value of the constant A, which increased from 405.7 to 435.4, 572.3, and 1055.0, for the increasing flow rates of 0.5 to 0.8, 1.5, and 2.4 mL/min, respectively.

3.4. Analysis of 1 L Sample at 5.0 mL/min. After confirming that a quantitative relationship between sensor response and *G. lamblia* concentration correlated well, an even higher flow rate (5.0 mL/min) was tested in a once-through flow mode for examining if a large 1 L sample could be analyzed. The purpose of using higher flow rate is to explore the possibility of large sample processing in a short time without a preconcentration step for detection. The frequency response of the sensor to 1,000 and 10,000 cysts in 1 L at 5.0 mL/min is given in Figure 5 and compared with the response obtained at lower flow rates. On an average, the resonant frequency decreased by 3,800 ± 895 Hz (n = 3) when 1 L of 10 cysts/mL *G. lamblia* was tested in a once-through fashion. And the response for 1 L of 1 cysts/mL *G. lamblia* was 1,950 ± 318 Hz (n = 3). The magnitude of sensor response is larger than the response obtained at lower flow rates, which is consistent with the trend shown in Figure 4. Control experiments were carried out with 10,000 cysts with an unfunctionalized sensor (no antibody, but gold coated) and the responses were 42 ± 24, 54 ± 36, 58 ± 24, 65 ± 21, and 194 ± 50 Hz at flow rate of 0.5, 0.8, 1.5, 2.4, and 5.0 mL/min, respectively. The higher response level at 5.0 mL/min may include some sensor drift as the length of experiment was longer than 4 h. One notes the sensor responses for 1,000 and 10,000 cysts at 5.0 mL/min are easily distinguishable

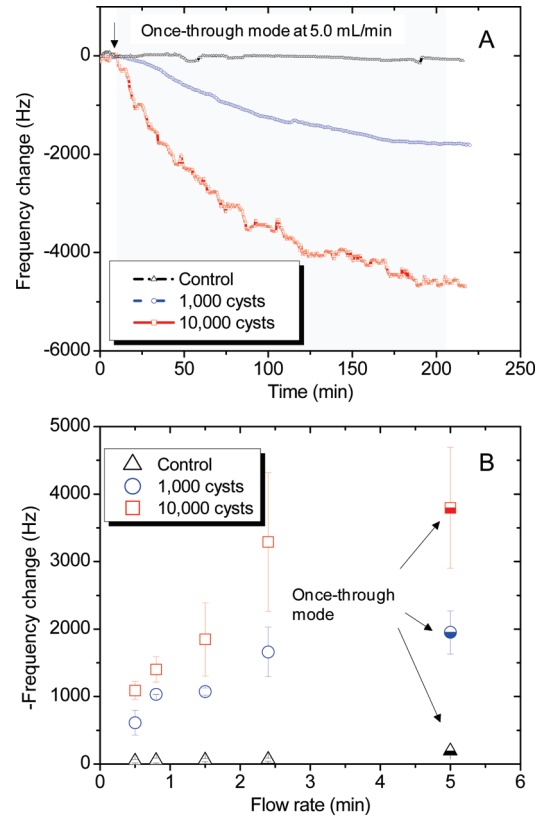

FIGURE 5. (A) Detection of 1 cyst/mL and 10 cysts/mL *G. lamblia* in 1 L sample at 5.0 mL/min. The 1 L sample containing either 1,000 or 10,000 cysts was introduced into the flow loop in a once-through mode followed by PBS rinse. Average responses for 1 and 10 cysts/mL were 1,950 ± 318 Hz and 3,800 ± 895 Hz, respectively. Control responses with 10,000 cysts were 380 ± 42 Hz. (B) PEMC sensors responses to 1,000 and 10,000 cysts as a function of flow rate. Once-through mode was used in detection at 5.0 mL/min, and the others were on a recirculation mode. Control experiments that exposed unfunctionalized sensor to 10,000 cysts were carried out at various flow rates. Error bars represent one standard deviation (n = 3–5).

from the controls. The tests showed detection feasibility of 1 cyst/mL in a 1 L sample in 4 h at 5.0 mL/min. The data in Figure 5A can be normalized by considering the arrival rate of target cysts at the sensor by plotting sensor response against $C \cdot t$ where C is cyst concentration and t is time. Such a plot (given in Figure S4) nearly merges the two response profiles into one suggesting that the binding rate when normalized for concentration were nearly the same.

The transport of cysts to the sensor surface is the first of a two-step process that leads to sensor response (*22*). The second step is the binding reaction to surface-immobilized antibody. It is also important to note that a cyst is non-spherical and thus flow velocity would increase its rotation which potentially could enhance exposure of binding site to immobilized antibody on sensor. The transport step is governed by the flow field in the flow cell. To examine the reason for higher response at higher flow rate, we examined two questions. Namely: Is the sample flow velocity sufficient in the flow cell to carry the cysts to sensor surface? Qualitatively what is the difference in the flow field at the two extreme flow rates used (0.5 and 5.0 mL/min)?

Stokes settling velocity of the cysts (assuming average diameter = 10 μm, density = 1.02 g/cm^3) is ~0.000109 cm/s, and the average velocity of fluid in the flow cell is 0.046–0.46 cm/s for the flow rate range of 0.5–5.0 mL/min. Thus the flow velocity is far greater than the settling velocity, and we expect the cyst to follow the fluid flow path through the flow

cell. To examine the second question, a calculation of the flow field in the flow cell using 2-D Navier−Stokes equation was conducted and the resulting flow maps are given in Figure S5. Finite element simulation (COMSOL Multiphysics, Boston, MA) at various flow rates from 0.5 to 5.0 mL/min were analyzed. The significant difference observed in the flow map was the extent of flow adjacent to the sensor surface at the two flow rates. The vertical velocities adjacent to sensor were extracted from the finite element calculation at three representative sensor surface locations, and are plotted as a function of distance from the sensor. At a distance of 100 μm from the middle point of the sensor (see Figure S5, point B), the vertical velocity was 0.044 cm/s at 5.0 mL/min, which is about 5 times greater than 0.009 cm/s at 0.5 mL/min. A distance of 100 μm is approximately 10 times the size of *Giardia* cysts, and to the first approximation is the region that the sensor samples. We believe that higher level of interaction of the sample with the sensor surface increases the probability of the cysts binding to it. Higher inlet velocity results in better exposure of *G. lamblia* cysts to the antibody on the sensor surface and accounts for the higher sensor response. Although an even higher flow rate can improve cysts interaction with the sensor surface, a higher noise level in resonant frequency occurs which compromises the measurement. Furthermore, higher flow rate will also cause higher surface shear stress at the sensor surface which potentially could dislodge bound cysts or impede binding of cysts to antibody.

3.5. Detection of G. lamblia in Tap Water and River Water. Having established detection feasibility at 1 cyst/mL in buffer background, we examined if similar sensitivity can be obtained in practical matrixes, namely tap and river waters. The first set of experiments was designed to examine if the tap and river water samples contained any *Giardia* cysts. Antibody-immobilized sensors exposed to 50 mL of tap/river water in a once-through mode after stabilization in DI water showed no detectable response, which verified that no cysts were present in the tap/river water tested. Negative controls in PBS, tap, and river water with antibody-immobilized sensors exposed to the three water samples showed 15 ± 6, 20 ± 5, and 39 ± 9 Hz response, respectively. Positive controls with unfunctionalized sensors exposed to 10,000 cysts spiked in the three water matrixes set in recirculation mode gave responses of 20 ± 5, 18 ± 8, and 45 ± 12 Hz, respectively (data not plotted). Sensors for detection experiments were functionalized with anti-*G. lamblia* and installed in flow cell with tap water or river water as running buffer. We used a flow rate of 2.4 mL/min as it gave low noise response, as seen in Figure 3. Spiked water samples containing 10−10,000 cysts were added to the flow loop following the same procedure as with the PBS samples. The results, summarized in Figure 6, show the response in tap water was 4−20% lower than in PBS and the response to river water samples was 20−47% lower at the concentrations tested. The control experiments verified that the positive responses to spiked samples were due to the cysts binding to sensor surface. We believe the lower sensor response compared to buffer samples is due to the interference of both biological and nonbiological matters in the sample matrix. Masking of binding sites of immobilized antibodies by organic molecules such as humic and fulvic acids in river water has been suggested in the literature (*14*). It is equally likely that antigenic sites on the cyst may weakly adsorb extraneous matter rendering then unrecognizable by surface-immobilized antibody. We believe the latter to be the dominant mechanism as our work on urine and serum samples show that proteinous matter in the sample matrix does not adsorb on PEMC sensors that are at resonance in a flow field (*23, 24*). However antigen-spiked samples did give a lower sensor response as we have found in the present study. Another factor that may also contribute

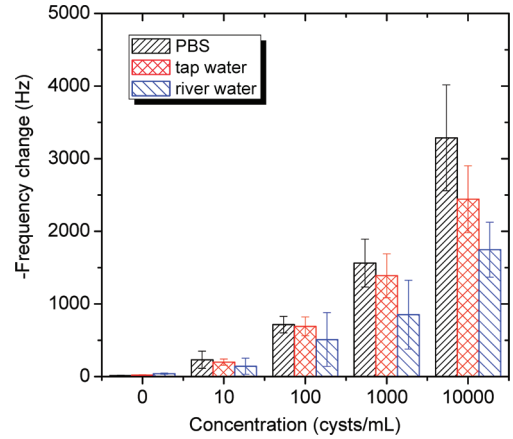

FIGURE 6. Comparison of sensor detection responses at 2.4 mL/min in the three water matrixes: PBS, tap water, and river water. In all cases sample size was 1 mL. Both tap and river water samples gave lower sensor response at the same concentration. The decrease of response is attributed to weak binding of materials in water to cysts surface. Error bars represent one standard deviation ($n = 4$).

to lower sensor response is the pH at which detection was carried out. The pH of tap and river waters was 6.7 ± 0.1 and 6.9 ± 0.1, respectively, and are lower than 7.4 at which the PBS experiments were conducted. In any case, the sensor exhibited sensitivity for detecting 10 cysts in tap and river water background. In practical situations, tap or river water samples can be diluted in PBS prior to detection for offsetting the observed reduction in sensor response. Since sample volume is not a limitation, detection sensitivity would not be compromised, but assay time will be lengthened.

Acknowledgments

We are grateful for the financial support from Environmental Protection Agency STAR Grant R833007.

Supporting Information Available

Detailed Materials and Methods section, experimental apparatus (Figure S1), sensor spectra in air and in flow cell at 5.0 mL/min and noise level due to increased flow rate (Figure S2), ESEM images of cysts attached to sensor surface (Figure S3), sensor resonant frequency response as function of $C \cdot t$ (Figure S4), and finite element simulation of the flow field in the flow cell at 0.5 and 5.0 mL/min (Figure S5). This material is available free of charge via the Internet at http://pubs.acs.org.

Literature Cited

(1) Adam, R. D. Biology of *Giardia lamblia*. *Clin. Microbiol. Rev.* **2001**, *14* (3), 447–475.

(2) Caccio, S. M.; Thompson, R. C. A.; McLauchlin, J.; Smith, H. V. Unravelling *Cryptosporidium* and *Giardia* epidemiology. *Trends Parasitol.* **2005**, *21* (9), 430–437.

(3) Savioli, L.; Smith, H.; Thompson, A. *Giardia* and *Cryptosporidium join the 'Neglected Diseases Initiative'*. *Trends Parasitol.* **2006**, *22* (5), 203–208.

(4) USEPA. Method 1623: *Cryptosporidium* and *Giardia* in water by filtration/IMS/FA; 2005.

(5) Rochelle, P. A.; DeLeon, R.; Stewart, M. H.; Wolfe, R. L. Comparison of primers and optimization of PCR conditions for detection of *Cryptosporidium parvum* and *Giardia lamblia* in water. *Appl. Environ. Microbiol.* **1997**, *63* (1), 106–114.

(6) Guy, R. A.; Payment, P.; Krull, U. J.; Horgen, P. A. Real-time PCR for quantification of *Giardia* and *Cryptosporidium* in environmental water samples and sewage. *Appl. Environ. Microbiol.* **2003**, *69* (9), 5178–5185.

(7) Rosenblatt, J. E.; Sloan, L. M.; Schneider, S. K. Evaluation of an enzyme-linked-immunosorbent-assay for the detection of *Giardia lamblia* in stool specimens. *Diagn. Microbiol. Infect. Dis.* **1993**, *16* (4), 337–341.
(8) Maraha, B.; Buiting, A. G. M. Evaluation of four enzyme immunoassays for the detection of *Giardia lamblia* antigen in stool specimens. *Eur. J. Clin. Microbiol. Infect. Dis.* **2000**, *19* (6), 485–487.
(9) Rule, K. L.; Vikesland, P. J. Surface-enhanced resonance Raman spectroscopy for the rapid detection of *Cryptosporidium parvum* and *Giardia lamblia*. *Environ. Sci. Technol.* **2009**, *43* (4), 1147–1152.
(10) Zhu, L.; Zhang, Q.; Feng, H. H.; Ang, S.; Chauc, F. S.; Liu, W. T. Filter-based microfluidic device as a platform for immunofluorescent assay of microbial cells. *Lab Chip* **2004**, *4* (4), 337–341.
(11) Li, X. X.; Cao, C.; Han, S. J.; Sim, S. J. Detection of pathogen based on the catalytic growth of gold nanocrystals. *Water Res.* **2009**, *43* (5), 1425–1431.
(12) Campbell, G. A.; Mutharasan, R. A method of measuring *Escherichia coli* O157: H7 at 1 cell/mL in 1 liter sample using antibody functionalized piezoelectric-excited millimeter-sized cantilever sensor. *Environ. Sci. Technol.* **2007**, *41* (5), 1668–1674.
(13) Campbell, G. A.; Mutharasan, R. Method of measuring *Bacillus anthracis* spores in the presence of copious amounts of *Bacillus thuringiensis* and *Bacillus cereus*. *Anal. Chem.* **2007**, *79* (3), 1145–1152.
(14) Poitras, C.; Fatisson, J.; Tufenkji, N. Real-time microgravimetric quantification of *Cryptosporidium parvum* in the presence of potential interferents. *Water Res.* **2009**, *43* (10), 2631–2638.
(15) Campbell, G. A.; Mutharasan, R. Near real-time detection of *Cryptosporidium parvum* oocyst by IgM-functionalized piezoelectric-excited millimeter-sized cantilever biosensor. *Biosens. Bioelectron.* **2008**, *23* (7), 1039–1045.
(16) Ogi, H.; Fukunishi, Y.; Omori, T.; Hatanaka, K.; Hirao, M.; Nishiyama, M. Effects of flow rate on sensitivity and affinity in flow injection biosensor systems studied by 55-MHz wireless quartz crystal microbalance. *Anal. Chem.* **2008**, *80* (14), 5494–5500.
(17) Ziegler, C. Cantilever-based biosensors. *Anal. Bioanal. Chem.* **2004**, *379* (7−8), 946–959.
(18) Maraldo, D.; Rijal, K.; Campbell, G.; Mutharasan, R. Method for label-free detection of femtogram quantities of biologics in flowing liquid samples. *Anal. Chem.* **2007**, *79* (7), 2762−2770.
(19) Huang, D. B.; White, A. C. An updated review on *Cryptosporidium* and *Giardia*. *Gastroenterol. Clin. North Am.* **2006**, *35* (2), 291–314.
(20) Campbell, G. A.; Mutharasan, R. Piezoelectric-excited millimeter-sized cantilever (PEMC) sensors detect *Bacillus anthracis* at 300 spores/mL. *Biosens. Bioelectron.* **2006**, *21* (9), 1684−1692.
(21) Maraldo, D.; Mutharasan, R. Detection and confirmation of staphylococcal enterotoxin B in apple juice and milk using piezoelectric-excited millimeter-sized cantilever sensors at 2.5 fg/mL. *Anal. Chem.* **2007**, *79* (20), 7636–7643.
(22) Squires, T. M.; Messinger, R. J.; Manalis, S. R. Making it stick: convection, reaction and diffusion in surface-based biosensors. *Nat. Biotechnol.* **2008**, *26* (4), 417–426.
(23) Maraldo, D.; Garcia, F. U.; Mutharasan, R. Method for quantification of a prostate cancer biomarker in urine without sample preparation. *Anal. Chem.* **2007**, *79* (20), 7683–7690.
(24) Rijal, K.; Mutharasan, R. PEMC-based method of measuring DNA hybridization at femtomolar concentration directly in human serum and in the presence of copious noncomplementary strands. *Anal. Chem.* **2007**, *79* (19), 7392–7400.

ES9033843